Human arm dynamics identification through experiments with KUKA Lightweight Robot 4+

Ricardo Alexandre Pereira Aniceto
ricardo.aniceto@tecnico.ulisboa.pt

Instituto Superior Técnico, Universidade de Lisboa, Lisboa, Portugal
December 2021

Abstract: Although human motor control studies have been done for over 100 years, still much is unknown in this area. The physiological mechanisms responsible for the force generation in the human joints are too complex, which makes the search for a mathematical model that describes these phenomena a problem without an exact solution. Nevertheless, the research of these phenomena is important for the understanding the human arm as a biomechanical system and may be beneficial for areas such as collaborative robotics, neuromuscular diseases research, motor rehabilitation and the development of limb prosthesis.

The work developed in this thesis is based on the identification of the human arm dynamics, taking into account the shoulder, the elbow and the wrist, through stochastic disturbances applied by the KUKA Lightweight Robot 4+ in the experimental subject's hand. One of the goals of this work is explore the different methods of disturbance used, which can be a disturbance of force or position. With experimental data acquired, a frequency domain analysis is employed and the dynamic behaviour of the arm is approximated to a 2nd order system. The main objective of this project is to validate the robotic system and the methods used for arm mechanical impedance estimation in multiple 3D directions. For that purpose, the estimated models of the dynamics of the human arm for each type of disturbance are compared together. Finally, the stiffness of the arm is estimated for different 3D directions, revealing the stiffness anisotropy of the human arm.

Keywords: human arm impedance identification, Musculoskeletal modelling, KUKA Lightweight Robot 4+, contraction dynamics, directional stiffness.

1. INTRODUCTION

Dynamics is the study of the forces applied to a body and the movement generated by them. This thesis focuses on the study of human arm dynamics and the methods used to estimate and model it. In this study, it is considered the shoulder, elbow, and wrist joints.

The main objective of this thesis is to validate the method used to identify the mechanical impedance of the human arm and make it feasible to perform these tests with the KUKA Lightweight Robot 4+. Other goals include verifying whether it is feasible to approach the human arm dynamics to a 2^{nd} order system and estimate the human arm impedance in different directions.

Although human motor control studies have been done for over 100 years, much is still unknown about the physiological mechanisms responsible for the movement generation. These mechanisms can be divided in two components: the neuronal component, which includes mechanisms such as the perception of the environment through the senses of the human body, the information processing, the decision-making process, and the signal sending process to the muscles; and the biomechanical component, which covers the physical components of the joints such as the muscles involved, bones, tendons, among others.

Due to the high complexity of the mechanisms involved in the generation of joint movement, it may not be possible to develop a mathematical model that fully describe these phenomena. Nevertheless, the research of these phenomena is important for the understanding of the human arm as a biomechanical system and may be beneficial for areas such as collaborative robotics, neuromuscular diseases research, motor rehabilitation and the development of limb prosthesis.

2. STATE OF THE ART

The first measurements of the human arm impedance were made by Mussa-Ivaldi, Hogan and Bizzi [1] in 1985. An experimental method was developed where the experimental subjects were asked to maintain the same posture while a force was applied to their hand, in different directions of a plane, through torque motors. The displacement and force applied to the hand were measured before there was a voluntary reaction by the subject. It was observed that the contribution of conservative forces was much higher than the contribution of non-conservative forces, therefore it was concluded that multiarticular behaviour was mainly elastic. Since the relationship between force and displacement was considered a linear relationship, stiffness was estimated in different directions of displacement. Thus, it was noticed that the estimated stiffness varied in the direction of the disturbance and the directional stiffness of the human arm was represented by an ellipse where the stiffness can be visualized in the different directions (fig. 1).

It was also concluded in this study that the magnitude, shape, and orientation of the stiffness ellipse vary with arm posture. These changes can be observed in [3]. In this study, tests were performed like the tests in [1], where a robot with two joints applied a stochastic position disturbance to the subject's hand and the resulting force

was measured. The subject was asked to apply a voluntary force in one direction. After that, it was computed a non-parametric estimation of the resulting dynamics and that estimation was approximated to a 2nd order model with the parameters of inertia, viscosity, and stiffness. It was observed that stiffness increases linearly as the voluntary force generated increases, and viscosity increases nonlinearly. Inertia did not change with the variation of the level of voluntary force. After parameterization, it was possible to estimate the damping coefficient and it was noticed that it was constant and was approximately equal to 0.26, thus being categorized as a sub-cushioned system.

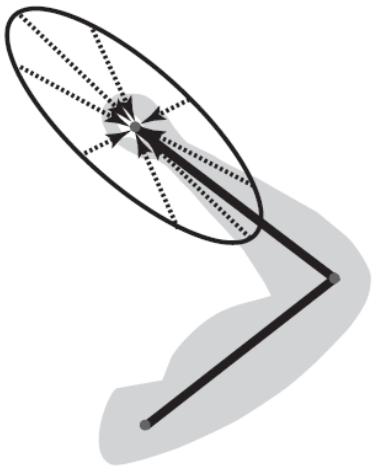

Fig. 1 – Stiffness ellipse [2].

3. KUKA LIGHTWEIGHT ROBOT 4+

The KUKA Lightweight Robot 4+, or LWR, is a robotic arm developed by KUKA Roboter GmbH in collaboration with the Institute of Robotics and Mechatronics at the German Aerospace Center [11]. The LWR has 7 rotating joints, which makes it redundant in the three-dimensional space. All joints have position and torque sensors, giving the robot the ability to be operated with position, velocity, or torque inputs. The robot is controlled through its controller, which is connected to a teach pendant operated by the user.

The interaction with the robot can be done through the KUKA Robot Language or through the Fast Research Interface (FRI). In this thesis, the FRI was used, since with this strategy it is possible to easily change the main control parameters, thus being more appropriate for the tests performed in this thesis.

FRI is an interface integrated in the LWR that allows the user to control the robot through an external computer in "real time". This interface was developed particularly for laboratory experiments [7].

A strategy similar to the strategy used by Žlajpah and Petrič in [11] was used. In this strategy, two additional computers are used, designated as host and target, presented in figure 2.

On the robot controller, an FRI file is initialized that has the function of configuring the connection with the target computer, receiving and sending the necessary data for the robot control.

On the host computer is implemented the server program in *Simulink* which is converted into a program in *C* programming language, compiled and is sent as *Simulink Real-Time* application to the target. It is also in the server program, on the host, where the user chooses the parameters of control used. On this computer is also implemented an animation to visualize the robot, the forces applied and the torque of each joint.

The target computer boots with the *Simulink Real-Time* operating system and has the function of running the application generated by the host. The host and the robot controller are connected to the target and, in order to ensure the required sampling time for a "real-time" communication, these connections are made via ethernet cables, with the UDP communication protocol. On the target screen, some data regarding the robot, such as the joint position, is displayed.

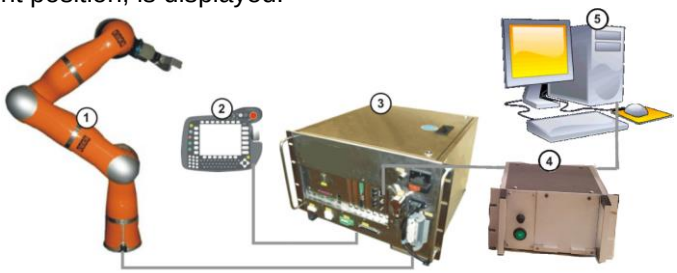

Fig. 2 – Experimental setup configuration [11]: 1) Robotic manipulator; 2) Teach pendant; 3) Robot controller; 4) Target computer; 5) Host computer.

The LWR has three control strategies available: joint position control, joint impedance control and cartesian impedance control. Cartesian impedance control is used in the tests performed in this thesis. In this strategy the robot moves with the cartesian position of the end effector as reference. The user can specify cartesian position and impedance. That is, the robot's behaviour resembles a system formed by six mass-spring-damper systems acting in different directions of motion (three directional and three angular dimensions). The mass of the analogous system is the apparent mass in the end effector and the stiffness and damping rate parameters are defined by the user. The control rule of equation 1 is followed.

$$\tau_{cmd} = J^T(k_{car}(x_d - x_r) + \beta_{car} + F_d) + f_{dyn}(q_d, \dot{q_d}, \ddot{q_d}) \quad (1)$$

Where J is the robot Jacobian, x_d and x_r are the desired and actual end effector cartesian positions, respectively, and F_d is the additional force given by the user. The matrix k_{car} and the vector β_{car} stiffness and damping, respectively, felt in the end effector. It is possible to define a different stiffness and damping for each of the six dimensions.

Because the robot is redundant in the three--dimensional space, there are several configurations of the robot that serve as a possible solutions to the reference position. This set of solutions is called null

space. Thus, there is a need to control this null space, which is done in a similar way to the joint impedance control. The position of the desired joints and the impedance of the null space, their stiffness and damping ratio are defined by the user.

If the stiffness of each direction is configured as zero, the robot enters a state of gravity compensation. That is, in this state the torque of the joints only compensates the robot's weight and the part of its inertia. In this state, the robot remains at rest if it has no disturbances, and it is easily moved with application outside forces.

In order to visualize the robot configuration, the torque generated in the joints and the force applied in the end effector, an animation was created in another *Simulink* file that is implemented and initialized on the host computer.

4. EXPERIMENTAL PROCEDURE

In the tests performed, the LWR is used to apply a disturbance to the arm which is at rest. For this, a part for connection between the robotic arm and the experimental subject's arm was 3D printed. This part can be designated as a simple handle screwed to the end effector of the robot and is held by hand by the experimental subject, as shown in figure 4.

The first step of the experimental procedure is to use the robot's position control and place the robot in the initial configuration required for the tests. After that, the control strategy is changed for the cartesian impedance control, where the position of the end effector, the stiffness and damping in the six spatial coordinates and the position, stiffness and damping of the null space are defined. Then, with the robot prepared for the experimental test, the subject is asked to sit in the chair and hold the handle by hand with the arm relaxed or contracted. Finally, a disturbance is applied for 30 seconds, and the data is collected and analysed.

As a disturbance for the tests, an emulation of white noise was used for a frequency range between 0.1 and 15 Hz, shown in Figure 4. This frequency range was chosen based on the assumption that the arm has a bandwidth of up to 10 Hz. This signal was obtained with a sum of sinusoids with a frequency within the defined range. The disturbance signal was applied in the reference position, x_d in the robot control algorithm in equation 1, or in the desired applied force, F_d in the same equation.

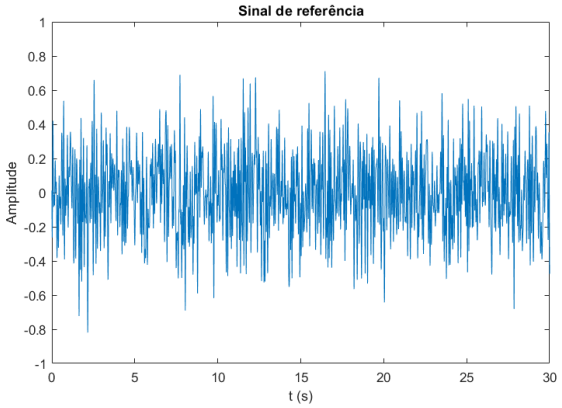

Fig. 3 – Reference disturbance signal with a unitary amplitude.

In a first stage, tests were performed without the presence of the arm, designated by free tests, to identify the system emulated by the robot. It is only after the free tests that the tests with the arm are performed. In the experiments with the arm, the user was asked to relax or contract the arm.

For this experimental procedure, security measures were implemented: in the FRI file, position, velocity, and force limiters are present; in the server program there are position interpolators that calculate the trajectory of the robot considering a maximum velocity defined by the user. In addition to these measures, there is a safety button on the teach pendant that locks all the robot joints and it is in the user's possession for the entire duration of the test.

5. DATA PROCESSING AND ANALYSIS

To identify the arm, first of all, an identification of the complete system of the tests is made. That is, it is identified the total system consisting of the simulated

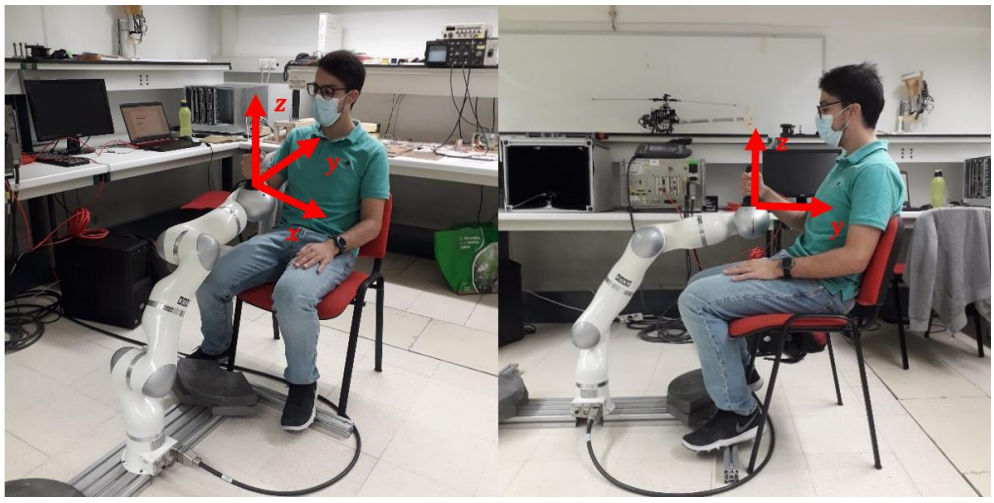

Fig. 4 – LWR and experimental subject during tests.the

system of the robot together with the arm. For this, a frequency domain identification is made of the relationship of the disturbance signal with the measured position signal.

To build a non-parametric model of the system, it is used the *matlab* function *tfestimate*. This function estimates a model of the frequency response of the system based on the relation between the cross-spectral density of the input and output signals, $S_{xy}(f)$ and the spectral density of the input signal, $S_{xx}(f)$, represented in equation 2.

$$H(f) = \frac{S_{xy}(f)}{S_{xx}(f)} \tag{2}$$

This estimated model is approximated to a 2nd order system using the *tfest* function. From the results of this process, it is possible to remove the parameters of the complete system such as stiffness, damping coefficient, inertia, natural frequency, damping ratio and static gain.

After the estimation of the models in the tests performed, the arm model is calculated from the subtraction of the contribution of the model of the system emulated by the robot, estimated in the free test, and the total system model, estimated in the tests with the arm. Assuming that the arm has a behaviour similar to a mass--spring-damper system, the system analogous to the tests performed with the arm is shown in figure 5. Equations 3 and 4 represent the transfer function of the analogous system for force and position disturbance, where M_r, k_r and β_r are the mass, stiffness, and damping coefficient of the arm, respectively, M_r, k_r e β_r are the same parameters for the system emulated by the robot, F is the force disturbance, x_0 is reference position disturbance and x is the measured position.

$$\frac{X(s)}{F(s)} = \frac{1}{\mathrm{k_r} + k_b} \frac{\frac{k_r + k_b}{M_r + M_b}}{s^2 + \frac{\beta_r + \beta_b}{M_r + M_b} s + \frac{k_r + k_b}{M_r + M_b}} \tag{3}$$

$$\frac{X(s)}{X_0(s)} = \frac{\frac{k_r}{M_r + M_b}}{s^2 + \frac{\beta_r + \beta_b}{M_r + M_b} s + \frac{k_r + k_b}{M_r + M_b}} \tag{4}$$

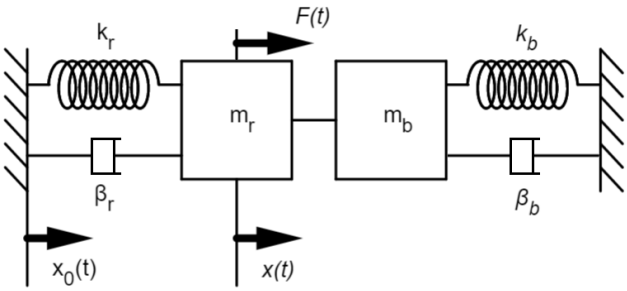

Fig. 5 – Analogous system of tests with the arm.

6. UNIDIRECTIONAL POSITION DISTURBANCE TESTS

Experiments were performed with three different cartesian stiffness levels in order to test the effect of the stiffness level of the simulated system in the arm dynamics model. Tests with simulated stiffness of 1500, 3000 and 4500 N/m were performed, with a damping ratio of 0.5, with disturbances with maximum amplitude of 1 cm and with a duration of 30 seconds in the direction x, represented in figure 4.

After the tests, it is made a frequency domain response estimation of the total system. Figure 6 shows the estimated response in frequency calculated in the test with an emulated stiffness of 3000 N/m performed with the arm relaxed and with the arm contracted compared to the estimate of the robot system in the free tests.

Note that the cut off frequency drops slightly from both the free test to the test with the relaxed arm and from the test with the relaxed arm to the test with the contracted arm. Since the cut off frequency depends on the stiffness and total mass of the system, it would be expected that the stiffness would increase from the free test to the test with relaxed arm and from the test with relaxed arm to the

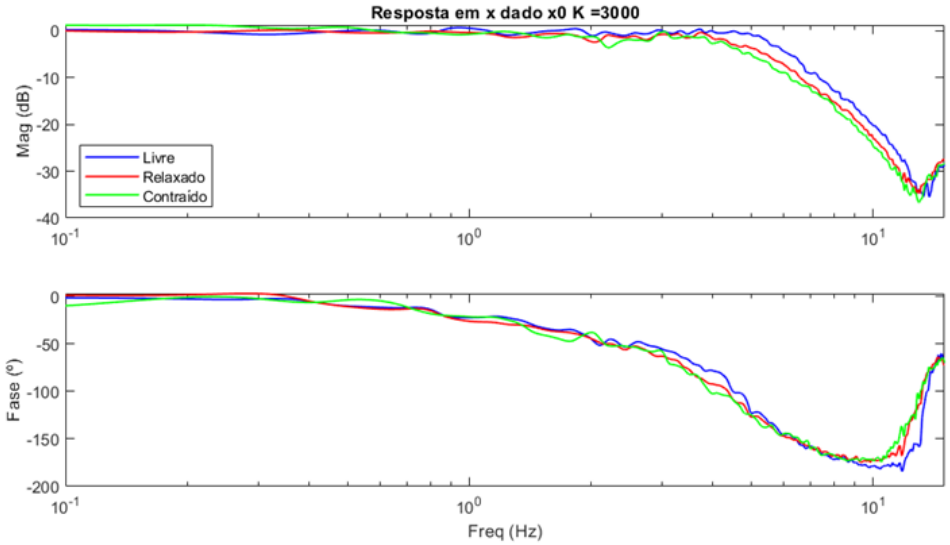

Fig. 6 – FRF of robot+arm system with position disturbance with K=3000 N/m.

with the contracted arm and, thus, it is expected an increase in the cut off frequency. However, this is not the case. Therefore, it is concluded that the increase in inertia in the system is more significant than the increase in stiffness. It is concluded that this inertia is not only related to the mass of the arm, because it does not change with the contraction of the arm since it would imply an increase in the mass of the arm, but rather with the behaviour of the experimental subject. That is, the arm appears to have a greater voluntary resistance to movement when contracted and hence the increase in inertia.

It is also expected that there would be a decrease in static gain since this parameter depends on the stiffness of the arm. This phenomenon occurs, however, it does not stand out since the simulated stiffness of the robot is much higher than the stiffness of the arm, being more noticeable in the test with a simulated stiffness equal to 1500 N/m.

After that, it was made an approximation to a 2nd order system of the results obtained in the tests with the arm, the component of the robot system is subtracted from the estimated system estimated and thus the arm dynamic models are obtained. The results of the approximation are presented in figures 9 and 10 and in table 1 together with the other methods.

As expected, there is an increase in the stiffness of the test with the relaxed arm to the contracted arm in all emulated stiffness values. In general, there was also an increase in inertia and damping coefficient, which may be explained by the behaviour of the experimental subject that tends to counter the movement imposed by the disturbance. For tests with the contracted arm, it is impossible for an experimental subject to maintain a stable and constant contraction level between the tests. Therefore, the quality of the method based on these tests cannot be compared. However, the relaxed arm is a more constant system and thus it is expected that the arm model will be similar for all tests regardless of the simulated stiffness used. It is also verified that the models estimated in the simulated stiffness tests equal to 3000 and 4500 N/m are very similar to each other but differ from the estimated model for the tests with K=1500 N/m. Given this, it is concluded that the method used is more consistent for higher simulated stiffness values.

7. UNIDIRECTIONAL FORCE DISTURBANCE TESTS WITH AN EMULATED IMPEDANCE

The tests with a force disturbance and a simulated impedance had the same procedure as the tests with position disturbance in one direction, however, the tests were performed for only one emulated stiffness value.

Tests with a simulated stiffness of 3000 N/m, a damping rate of 0.5 and a maximum disturbance amplitude of 30 N with a duration of 30 seconds were performed. These tests are similar to the tests with a simulated stiffness of 3000 N/m, changing only the type of disturbance. Note that the force disturbance of 30 N is equivalent to the position disturbance of 0.01 m with 3000 N/m of stiffness.

In figure 7, it is presented the estimated frequency response of the system in the free test overlapped with the estimations made for the tests with the arm. As with position disturbance tests, the cutting frequency drops from the free test to the test with the arm relaxed and descends once again to the test with the contracted arm. There is also a decrease in static gain, as expected by equation 3. Note that these results are very similar to the results obtained in the disturbance of position.

After that, the arm model was obtained as was done in the previous method. The results of the approximation are presented in figures 9 and 10 and in table 1.

Once again, there is an increase in stiffness, damping coefficient and inertia of the contracted arm in relation to

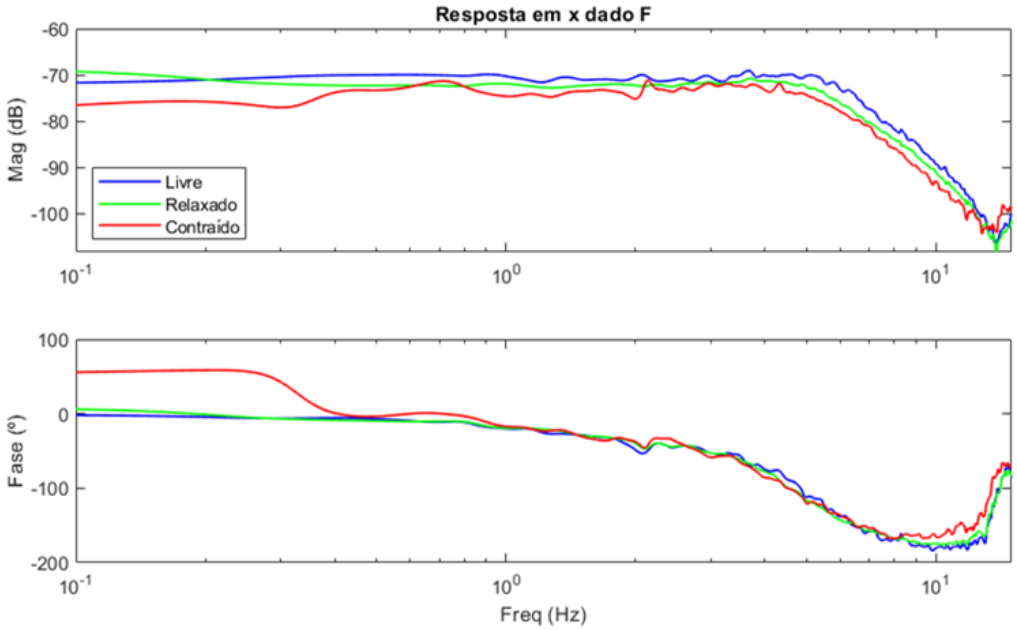

Fig. 7 – FRF of robot+arm system with force disturbance with K=3000 N/m.

the relaxed arm. However, the natural frequency and damping rate are very similar between the two tests, as there is a proportional increase in stiffness, damping and inertia from the relaxed arm to the contracted arm.

8. UNIDIRECTIONAL FORCE DISTURBANCE TESTS WITHOUT AN EMULATED IMPEDANCE

The next tests were performed with force disturbance, but without an emulated impedance of the robot. That is, the robot was placed in a gravity compensation mode and, from there, the force disturbance was applied to the experimental subject's arm. The gravity compensation mode does not completely compensate the inertia of the robot and the friction in the joints, however these components can be disregarded in the model analysis. Consequently, in this situation, the force is applied directly to the arm and the arm dynamics model is obtained directly without the need to subtract the emulated model from the robot.

When the robot is in gravity compensation, it is necessary that the subject exercises some force to keep the arm fixed. Thus, it is not possible to keep the arm completely relaxed in these tests. Two tests were performed in this phase of testing: one with a disturbance amplitude equal to 10 N, which implies a low contraction level of the experimental subject, and the other with an amplitude of 20 N, where a maximum contraction of the subject was requested. For the purposes of presentation results, the tests are designated as "semi-contracted" and contracted respectively.

In figure 8, it is presented the estimation of the frequency domain response made in the two tests. In these tests, it is verified that the estimated model of the arm is very similar to a 2nd order system, therefore validating the initial hypothesis of approximating the arm dynamics model to this type of system. Thus, it would be expected that the cutting frequency would increase and the static gain decreased with the increase in stiffness caused by the increase in the level of contraction of the arm. Through observation of figure 8, it is verified that these two phenomena are confirmed in the tests performed.

After that, the estimated models were approached to a 2nd order system with the function *tfest*. This system corresponds to the arm dynamics model. The results of the approximation are presented in figures 9 and 10 and in table 1.

It is verified a decrease in the inertia of the model from the semi-contracted test for the contracted test. There is also a proximity between the results of the model of the contracted arm from the tests with force disturbance without emulated impedance and the tests with the position disturbance with simulated stiffness equal to 1500 N/m.

9. SUMMARY OF UNIDIRECTIONAL TESTS

After obtaining all the results from the unidirectional tests, all models were organized in a table 1 and figures 9 and 10. In figure 9, it is presented all models of the relaxed arm dynamics, or semi-contracted in the case of the force disturbance test without an emulated impedance. In figure 10, it is presented the models of the contracted arm dynamics.

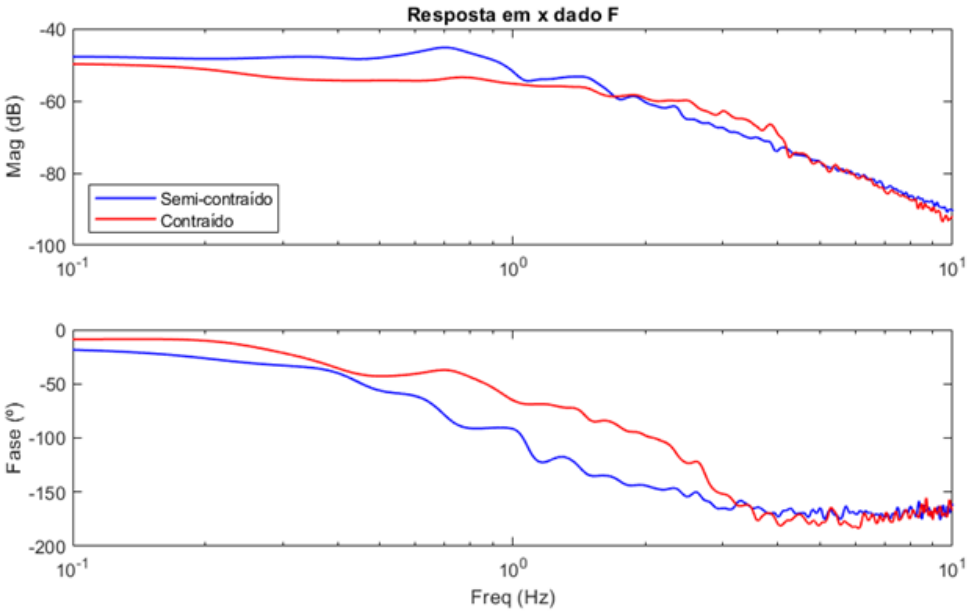

Fig. 8 – FRF of arm dynamics in force disturbance test without emulated impedance.

Table 1 – Estimated parameters of arm impedance.

Test			M_b (Kg)	β_b (N s/m)	k_b (N/m)	ω_n (Hz)	ξ	K_0 (x10^{-3})
Position disturbance	K =1500 N/m	Relaxed	0.912	11.01	65.75	1.35	0.71	15.2
		Contracted	1.389	26.72	451.46	2.87	0.53	2.21
	K=3000 N/m	Relaxed	1.752	43.28	601.39	2.95	0.67	1.66
		Contracted	2.319	54.65	716.89	2.80	0.67	1.39
	K=4500 N/m	Relaxed	1.657	45.86	493.12	2.75	0.80	2.03
		Contracted	2.323	57.34	731.17	2.82	0.70	1.37
Force dist.	K=3000 N/m	Relaxed	1.493	26.32	720.9	3.50	0.40	1.39
		Contracted	2.654	53.23	1343.7	3.58	0.44	0.74
	K=0 N/m	Semi-contracted	7.887	52.63	227.8	0.85	0.62	4.39
		Contracted	4.424	75.07	442.8	1.59	0.84	2.26

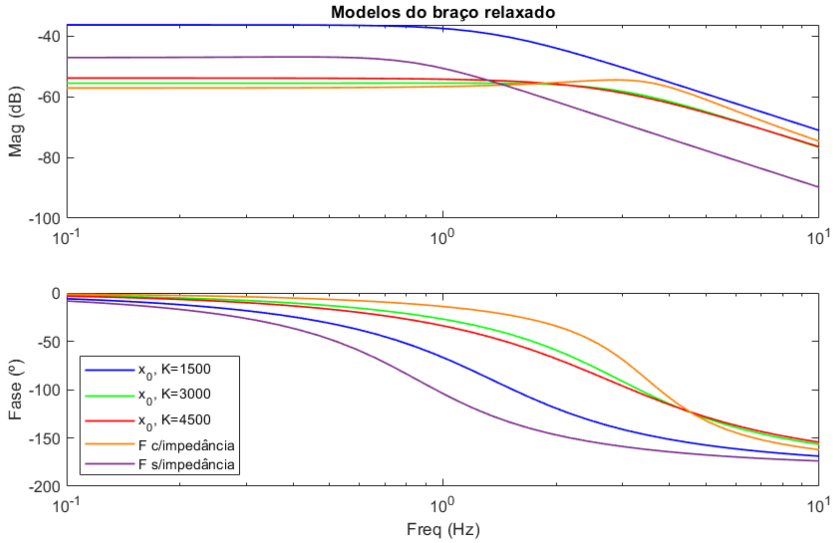

Fig. 9 – FRF estimated of relaxed arm.

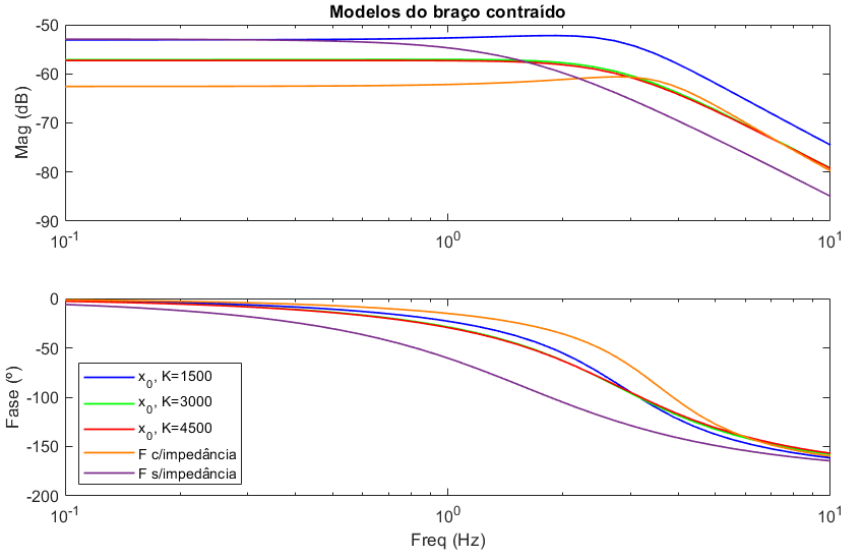

Fig. 10 – FRF estimated of contracted arm.

The most coherent methods between one another are the models from the tests with position disturbance with simulated stiffness of 3000 and 4500 N/m. Both models of the relaxed and contracted arm, estimated through these methods, are very similar, being almost indistinguishable in the case of the models of the contracted arm. From the Bode diagrams, it is also verified that similar arm dynamics models are obtained through the tests with force disturbance with an emulated impedance of the robot.

As expected, in almost all the methods used there is an increase in inertia, damping coefficient and stiffness of the relaxed arm model to the contracted arm model. The exception occurs in the models obtained in the test with force disturbances without an emulated impedance, where the estimated inertia was higher in the semi-contracted arm model. In the position disturbance test models with simulated stiffness of 3000 and 4500 N/m and in the force disturbance test with impedance models, it is verified that the natural frequency and damping ratio have close values between the relaxed and contracted arm model. In the other two methods, this phenomenon is not verified.

10. THREE-DIMENSIONAL POSITION DISTURBANCE TESTS

Finally, tests were performed with three different position disturbances in the three cartesian directions. As in the first tests performed, a free test and two tests with the arm were performed, one of them with the arm relaxed and the other contracted. The emulated stiffness in these tests was 3000 N/m, the damping ratio equal to 0.5, the disturbance had a maximum amplitude of 1 cm in the three cartesian directions and a duration of 30 seconds. The purpose of these tests is to estimate the directional stiffness of the arm.

The directional stiffness of the arm was calculated in a similar way to the method used in the position disturbance tests in one direction. The non-parametric model of the free test and arm test were made, these models were approximated to a 2nd order system without zeros and the robot system was subtracted from the total system of the tests with the arm. This process was repeated to calculate the stiffness of the arm for several directions, where the input signal and the output signal of the various directions were calculated based on the input and output data of the three cartesian directions

In figure 11, it is presented the representation of the calculated directional stiffness of the relaxed arm and the contracted arm in plane $z = 0$. In figures 12 and 13, it is presented the same stiffness in the three-dimensional space, where red colour is added in the zones of maximum stiffness, yellow in the medium zones and green in the zones of minimum stiffness.

From figure 11, it is not observed a stiffness ellipse, but it is verified a maximum direction of stiffness and, in a direction perpendicular to the direction of maximum stiffness, a direction of minimum stiffness, thus forming a shape similar to a "peanut". From figures 12 and 13, it is also verified the "peanut" shape in three-dimensional space. It should also be noted that the stiffness of the arm increases in all directions with its contraction, with a greater increase in stiffness in the directions of maximum stiffness.

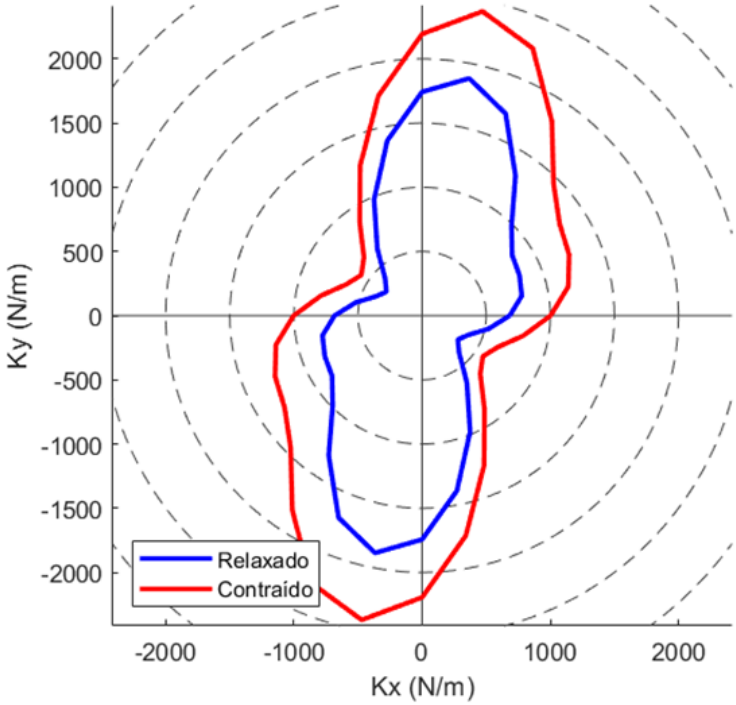

Fig. 11 – Directional stiffness of the arm relaxed and contracted in the plane $z = 0$.

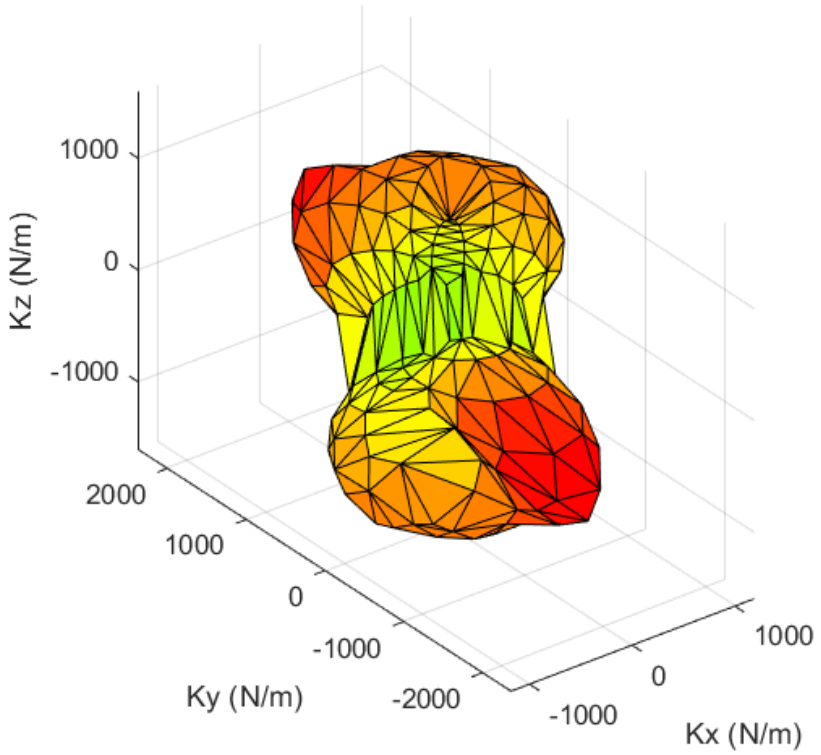

Fig. 12 – Directional stiffness of the relaxed arm in a three-dimensional space.

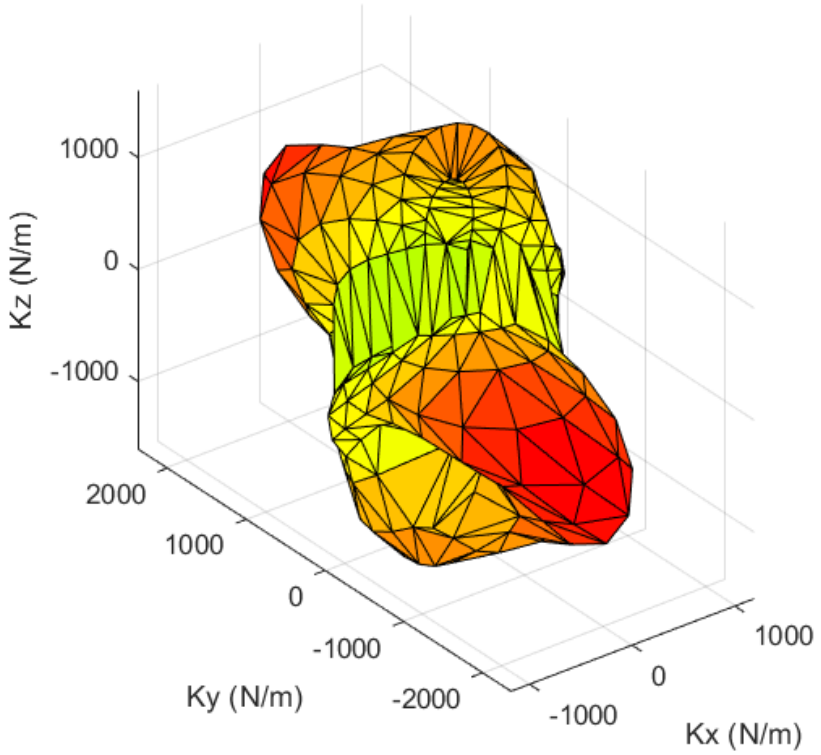

Fig. 13 – Directional stiffness of the contracted arm in a three-dimensional space.

11. CONCLUSION

The first stage of this project was the preparation of the experimental configuration for the tests: to connect the robot to an external computer, to develop a *Simulink* program to control the robot, to explore the control techniques available, to build the connection between the arm and the robot part and to define the experimental procedure.

With the experimental configuration prepared, it was defined the experimental tests to be done in order to create an arm model, to verify whether the approach of the arm to a 2nd order system is feasible and to estimate the directional stiffness of the arm. Therefore, position disturbance tests were performed in one and in all three directions and force disturbance tests were performed in one direction.

In the unidirectional position disturbance tests, the effects of the variation of the stiffness of the robot simulated system on the estimated arm model were studied. In this phase, the tests were performed with three different perturbations. It was verified that, for higher stiffness values, the estimated arm model became more constant.

In the next phase, tests with force disturbance with and without emulated impedance by the robot were performed. In the tests with an emulated impedance, a test similar to the test to the position disturbance tests was performed. Giving that, it would be expected that the results of the force disturbance tests with emulated impedance were similar to those of the position disturbance tests. There was a proximity between the tests results with the two types of disturbance and it was concluded that both types of disturbance were valid in identification of human arm dynamics.

In the force disturbance tests without an emulated impedance, the force is applied directly to the arm and, thus, there is no need to subtract an emulated dynamics from the robot, like with the other methods, and the arm dynamics are obtained directly. From the results of these trials, it was concluded that the approximation of the arm to a 2nd order system is feasible for the range of values analysed. However, the results obtained from this method were not as coherent as the previous methods. This may be due to the fact that the inertia and friction of the robot has been disregarded.

The last tests performed were the tests with position disturbance in three directions simultaneously. These tests aimed to estimate the stiffness ellipse, or an ellipsoid in the three-dimensional space. Therefore, the method used in the first tests was applied to estimate the human arm dynamics model in several directions. In the plane, a stiffness ellipse was not identified, but rather a stiffness in the form of a "peanut", with a maximum direction of stiffness and a perpendicular direction with minimal stiffness. The same could be verified in three-dimensional space.

Bibliography

[1] Mussa-Ivaldi, F. A., Hogan, N., Bizzi, E., Neural, mechanical, and geometric factors subserving arm posture in humans, The Journal of Neuroscience, 5: 2732–2743, 1985.

[2] Burdet, E., Franklin, D. W., Milner, T. E., Human Robotics: Neuromechanics and Motor Control, MIT Press, Cambridge, Massachusetts, London, England, 2013, ISBN 978-0-262-01953-8.

[3] Perreault, E.J., Kirsch, R.F., Crago, P.E. Multijoint dynamics and postural stability of the human arm. Experimental brain research, 157: 507–517, 2004.

[4] Gomi, H., Kawato, M. Human arm stiffness and equilibrium-point trajectory during multi-joint movement, Biological cybernetics, 76: 163-171, 1997.

[5] Tee, K., Burdet, E., Chew, C., A model of force and impedance in human arm movements. Biological cybernetics, 90: 368-375, 2004.

[6] Kearney, R. E., Hunter, I. W., System identification of human joint dynamics. Critical Reviews in Biomedical Engineering, 18(1): 55-87, 1990.

[7] KUKA System Technology, KUKA system software 5.6 lr – operating and programming instructions for system integratiors, 2010.

[8] KUKA System Technology, KUKA Fast Research Interface 1.0 – For KUKA System Software 5.6 lr, 2011.

[9] KUKA System Technology, KR C2 lr – Specification, 2012.

[10] KUKA System Technology, Lightweight Robot 4+ – Specification, 2012.

[11] R. Bischoff, J. Kurth, G. Schreiber, R. Koeppe, A. Albu-Schaffer, A. Beyer, O. Eiberger, S. Haddadin, A. Stemmer, G. Grunwald and G. Hirzinger, The KUKA-DLR lightweight robot arm - a new reference platform for robotics research and manufacturing, ISR 2010, ROBOTIK 2010, pp. 1-8, 2010.

[12] Žlajpah, L., Petrič, T., FRI-xPC server for KUKA FRI controller, IJS Technical report 11546, “Jožef Stefan” Institute Ljubljana, Eslovénia, 2014.

[13] Tejado, I., Valério, D., Pires, P., Martins, J., Fractional order human arm dynamics with variability analyses, Mechatronics, 23(7): 805-812, 2013.